# Reversible On/Off Switching of Lactide Cyclopolymerization with a Redox-Active Formazanate Ligand

de Vries, Folkert; Otten, Edwin

*Published in:*
ACS Catalysis

*DOI:*
10.1021/acscatal.1c05689



*Publication date:*
2022

ACS Catalysis

pubs.acs.org/acscatalysis

Letter

# Reversible On/Off Switching of Lactide Cyclopolymerization with a Redox-Active Formazanate Ligand

Folkert de Vries and Edwin Otten*

Cite This: *ACS Catal.* 2022, 12, 4125−4130

Read Online

ACCESS | Metrics & More | Article Recommendations | Supporting Information

**ABSTRACT:** Redox-switching of a formazanate zinc catalyst in ring-opening polymerization (ROP) of lactide is described. Using a redox-active ligand bound to an inert metal ion ($Zn^{2+}$) allows modulation of the catalytic activity by reversible reduction/oxidation chemistry at a purely organic fragment. A combination of kinetic and spectroscopic studies, together with mass spectrometry of the catalysis mixture, provides insight in the nature of the active species and the initiation of lactide ring-opening polymerization. The mechanistic data highlight the key role of the redox-active ligand and provide a rationale for the formation of cyclic polymer.

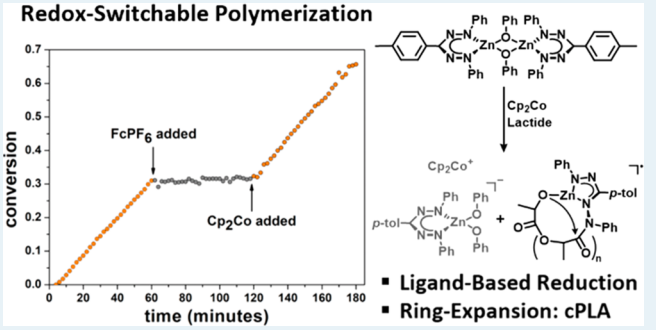


**KEYWORDS:** *catalysis, polymerization, cyclic polylactide, redox-switching, formazanate, redox-active ligand*



The synthesis of polymers with tailored properties is made possible by advances in catalysis and postfunctionalization methods to control polymer length, composition, and microstructure. Still, synthetic polymer chemistry pales in comparison to the sophistication achieved in nature's biopolymers.[1] Despite remarkable developments in polymerization methods, it has been difficult to exert spatial and/or temporal control, a key characteristic of biological systems to maintain homeostasis. One way to achieve this is by using catalysts that are responsive to electro-, photo-, or mechanochemical stimuli,[2] providing access to two (or more) states that have distinct reactivity. Wrighton's pioneering work on redox-switchable Rh hydrogenation catalysis[3] laid the foundation for the development of complexes that change activity in response to a redox stimulus. In the field of polymerization catalysis, switching of lactide ring-opening polymerization (ROP)[4] activity via redox chemistry was first described by Gibson and Long (Chart 1a).[5] This initiated the search for catalysts that provide precise spatiotemporal control of ROP for lactide and other cyclic esters to obtain advanced polymer architectures. An important class of redox-switchable ROP systems is developed by the Diaconescu group using ferrocene-linked chelating ligands (Chart 1b).[6] In addition to on/off switching, these catalysts also show oxidation-state-dependent monomer selectivity, providing unique block copolymers from a monomer mixture.[7] Byers et al. developed iron bis(alkoxide) complexes (Chart 1c) that show markedly different reactivity toward cyclic esters in the Fe(II) and Fe(III) states,[8] and several other redox-switchable ROP catalysts are known.[9−11] To date, switchable ROP of cyclic esters often relies on metal-based reduction/oxidation either at the "active" central metal or an Fc moiety in the ligand. Redox reactions at nonmetal sites have been much less explored.[12] Here, we demonstrate an approach that capitalizes on the redox chemistry of a purely organic ligand directly attached to a redox-inactive Zn center. Taking inspiration from the work of Coates and Chisholm on $\beta$-diketiminate (BDI) Zn and Mg complexes for lactide ROP,[13,14] we envisioned that using a

**Chart 1. Representative Examples of Catalysts Used in Redox-Switchable Polymerization of Lactide**

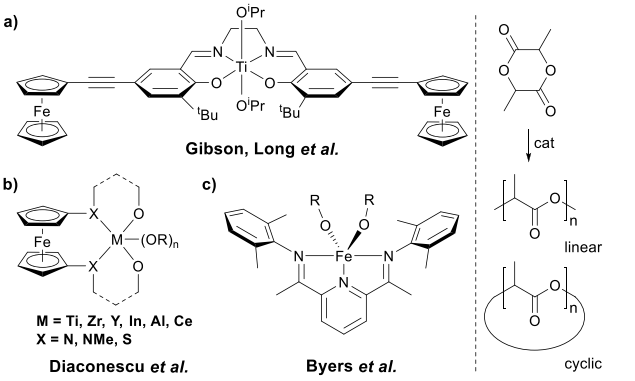


Received: December 10, 2021
Revised: February 18, 2022
Published: March 21, 2022

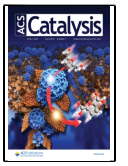

formazanate ligand[15] as a redox-active analogue to the well-known BDIs would impart redox-switching behavior to an otherwise inert catalyst. We demonstrate that this strategy indeed leads to an ROP catalyst that can be switched reversibly between "on" and "off" states using redox chemistry and discuss spectroscopic/kinetic data that corroborates the key role of the formazanate ligand in the switching process as well as the formation of cyclic polylactide (cPLA). Such polymers are of interest due to their distinct physicochemical properties.[16] To the best of our knowledge, this represents the first example of redox-switchable catalytic synthesis of cPLA.

As a starting point for this research, we prepared the formazanate zinc phenoxide **2** by protonolysis of **1**[17] (Scheme 1). X-ray diffraction revealed that complex **2** exists as a dimer

**Scheme 1. Synthesis of Compound 2 by Protonolysis**

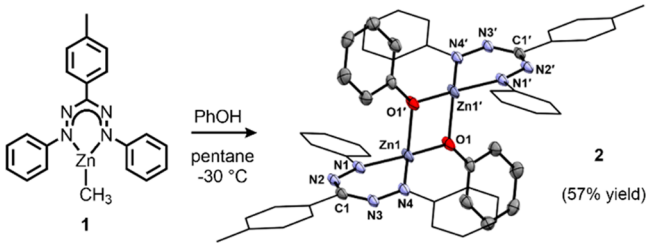


in the solid state, with tetrahedral Zn centers bridged by the phenoxides. Diffusion-ordered NMR spectroscopy in $CD_2Cl_2$ indicates that **2** retains a dimeric structure also in solution.

The cyclic voltammogram of **2** in THF shows two sequential, closely spaced reductions ($E_{1/2} \approx -1.45$ and $-1.63$ V vs $Fc^{0/+}$, Figure S8), which are assigned to the formation of the radical anion $\mathbf{2}^{\bullet-}$ and the dianion $\mathbf{2}_{2-}$, respectively. The close spacing and quasireversible nature of both redox couples suggests that all species remain dimeric at least on the time scale of the CV experiment. In $CH_2Cl_2$, a single (overlapping) redox wave is observed with a midpoint potential of $\sim -1.61$ V vs $Fc^{0/+}$ (Figure S9).

Turning to ROP catalysis, we found that **2** showed negligible reactivity toward *rac*-lactide (50 equiv) after 12 h in $CH_2Cl_2$ (Table 1, entry 1). This is in stark contrast to related (BDI)Zn catalysts by Coates, which are highly active.[13] However, addition of the reductant $Cp_2Co$ to the solution of **2**/lactide (1 equiv of $Cp_2Co$ per Zn center in **2**; [Co]:[Zn] = 1) turned on ROP activity, and 94% conversion of lactide was reached in 4 h

**Table 1. Polymerization of *rac*-Lactide Catalyzed by Formazanate Zinc Alkoxide Complex 2**[a]

| entry | [LA]:[Zn] | [Co]:[Zn] | conv. (%) | time (h) | $M_n$[b,c] | $M_w$[b,c] | $Đ_M$[d] |
|---|---|---|---|---|---|---|---|
| 1 | 50:1 | - | <1 | 12 | n.d. | n.d. | n.d. |
| 2 | 50:1 | 0.5 | 93 | 19 | 12.9 | 24.6 | 1.9 |
| 3 | 50:1 | 1 | 94 | 4 | 6.5 | 11.4 | 1.8 |
| 4 | 50:1 | 2 | 97 | 2 | 5.9 | 9.5 | 1.6 |
| 5 | 50:1 | 4 | 97 | 1 | 4.6 | 7.2 | 1.6 |
| 6 | 100:1 | 1 | 97 | 4 | 11.5 | 21.0 | 1.8 |
| 7 | 250:1 | 1 | 98 | 14 | 14.6 | 25.4 | 1.7 |
| 8 | 500:1 | 1 | 90 | 14 | 17.1 | 28.6 | 1.7 |

[a]Conditions: [**2**] = 5 mM, 25 °C, 1,3,5-trimethoxybenzene as internal standard, $CD_2Cl_2$ solvent; n.d. = not determined. [b]Reported in $10^3$ g $mol^{-1}$. [c]Determined by GPC in THF, calibrated versus polystyrene standards. [d]$Đ_M = M_w/M_n$ (see also ref 23).

(entry 2). A control experiment with lactide and $Cp_2Co$ or $[Cp_2Co][PF_6]$ in the absence of **2** shows no activity. Thus, $Cp_2Co$ converts inactive **2** into a reduced species that is catalytically active for lactide ROP. Monitoring the reaction by NMR spectroscopy shows a linear increase in monomer conversion, which indicates a rate law that is zero-order in lactide. It should be noted that metal-catalyzed ROP of cyclic esters is commonly first-order in monomer,[18,13b,19] but precedent for zero-order behavior exists.[20,21] The order in catalyst was evaluated by varying the total Zn concentration between 5 and 20 mM (at a constant [Co]:[Zn] ratio of 1). A plot of $\ln(k_{obs})$ vs $\ln([Zn]_{tot})$ afforded a slope of 0.53 (Figure S15). The half-order in $[Zn]_{tot}$ implies that most of the catalyst is present as an inactive dimer, while the active species is monomeric.[22]

Analysis of the polylactide product (after repeated precipitation from $CH_2Cl_2$/hexane) by NMR spectroscopy did not show the presence of the expected end group (OPh) nor did it contain resonances attributable to the formazan fragment. The MALDI-TOF spectrum contains signals for a polymer with a repeat unit of 72 Da (half a lactide monomer), with a major peak distribution that has the composition of $(lactide)_n + Na^+$(Figure S27). The absence of OPh end groups indicates that in our system the initiation of lactide ROP does *not* occur by nucleophilic attack of the Zn phenoxide; instead, the polymer produced by **2**/$Cp_2Co$ has a cyclic structure.[16a,b] This was corroborated using a derivative of **2** with a Zn−O$^i$Pr group instead of −OPh, which afforded a polymer with an identical mass spectrum.

The nature of the active species generated from **2** and $Cp_2Co$ was subject to further investigation. Specifically, it is notable that electrochemical reduction of **2** occurs at a more negative potential than that of $Cp_2Co$ ($E_{1/2} = -1.33$ vs $Fc^{0/+}$ in $CH_2Cl_2$).[24] Given the redox potentials, reduction of **2** by $Cp_2Co$ is likely incomplete when using [Co]:[Zn] = 1. However, in the presence of lactide, the CV shows an additional redox wave at more negative potential, which indicates that (as expected) the reduction product of **2** reacts with lactide (*vide infra*) and shifts the equilibrium. We subsequently monitored the conversion of *rac*-lactide via $^1$H NMR spectroscopy in $CD_2Cl_2$ with increasing [Co]:[Zn] ratios. The result is an approximately linear increase in the reaction rate (Figure 1A), which we ascribe to a higher (equilibrium) concentration of the active catalyst upon increasing the $Cp_2Co$ concentration. GPC analyses of polymers obtained with different amounts of reductant show that $M_n$ decreases, and a narrower molecular weight distribution is obtained at higher [Co]:[Zn] ratios (Table 1, entries 2−5), which is in line with an increase in the amount of active catalyst. Doubling the amount of lactide led to an approximate 2-fold increase in $M_n$ and $M_w$ (Table 1, entries 3 vs. 6). Further increasing the lactide:[Zn] ratio to 250:1 and 500:1 results in higher molecular weights (entries 7 and 8). The increased viscosity for reaction mixtures with high lactide concentration likely results in mass transfer limitations and lower molecular weights than expected.

EPR spectroscopy provided additional evidence for the proposed redox equilibrium. Data were collected in $CH_2Cl_2$ in the absence of lactide but using the same concentration of **2** and [Co]:[Zn] ratios as in the catalysis experiments.

The room-temperature EPR spectra show a broad signal at $g \approx 2$ as expected for an organic (ligand) radical (Figure 1B).[25] Double integration of this signal shows that its intensity


https://doi.org/10.1021/acscatal.1c05689
ACS Catal. 2022, 12, 4125−4130

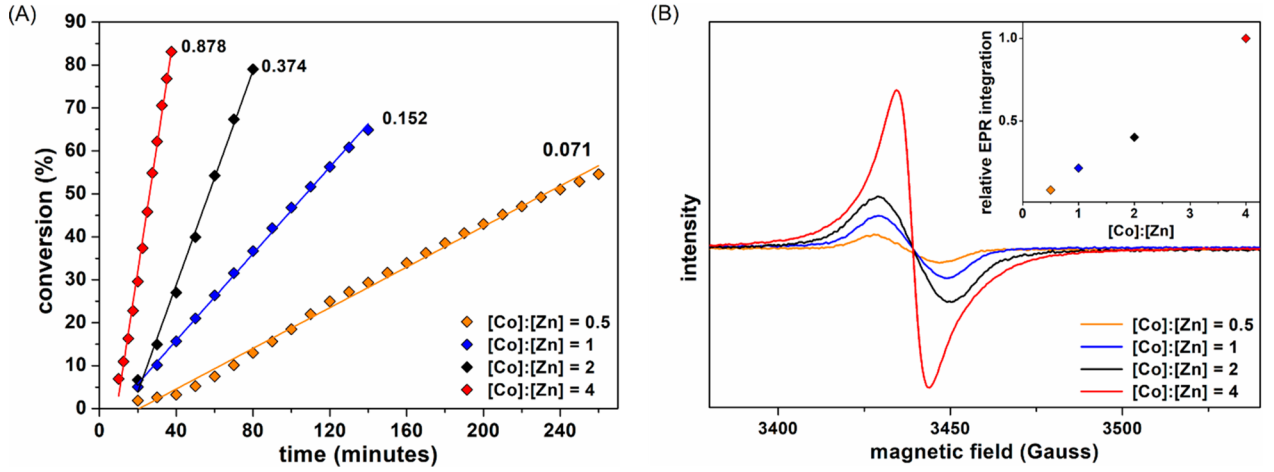


**Figure 1.** (A) Plot of monomer conversion vs time using **2** with various ratios of [Co]:[Zn] ($CD_2Cl_2$, 25 °C, $[LA]_0/[Zn]$ = 50, [Zn] = 10 mM). The numbers in the graph correspond to the observed rate constant ($M{\cdot}h^{-1}$). (B) Room-temperature X-band EPR spectra of **2** (5 mM in $CH_2Cl_2$) with varying amounts of $Cp_2Co$ added; inset shows the relative double integrations of the EPR spectra with varying [Co]:[Zn] ratios.

increases linearly with the [Co]:[Zn] ratio, in the same way as that the reaction rate increases. To achieve quantitative conversion of **2** to the catalytically active species, we reacted it with the stronger reductant $Cp^*_2Co$ ($E_{1/2}$ = −1.94 V vs $Fc^{0/+}$).[24] Although the catalytic activity of **2**/$Cp^*_2Co$ was indeed generally higher than with $Cp_2Co$, the rates were somewhat variable. This may be related to detrimental side reactions with the Cp* Me groups (e.g., CH deprotonation)[26] as observed in related iron formazanate chemistry.[27] The UV/vis absorption spectrum of **2** in $CH_2Cl_2$ shows a strong absorption in the visible region ($\lambda_{max}$ = 549 nm; $\varepsilon$ = 33 500 $M^{-1}$ $cm^{-1}$) characteristic for the $\pi-\pi^*$ transition of formazanate ligands.[17,28] Addition of either *rac*-lactide, $Cp_2Co$, or both results in small changes (see SI), but a low-energy band ($\lambda$ > 750 nm) characteristic for one-electron reduced formazanate complexes[15] is either absent or too weak to be observed due to its low equilibrium concentration. Treatment of **2** with $Cp^*_2Co$ does result in appearance of an absorption band at $\lambda \approx$ 775 nm (Figure S26), indicating that ligand-based reduction of **2** is indeed feasible. Attempts to isolate the putative reduction product $\mathbf{2}^{\bullet-}$ were unsuccessful; instead, the salt $[Cp^*_2Co]^+[LZn(OPh)_2]^-$ (**A**; L = formazanate; Scheme 2) was obtained by crystallization (see SI for the X-ray structure).

Mass spectrometry by direct injection of a polymerization reaction mixture during turnover showed a repeating unit of 72 Da, but different than for the polymers isolated after workup (*vide supra*), we now observe a distribution that indicates an "initiator" of 377.03 Da (Figure S27). This corresponds well with the calculated mass of the (formazanate)Zn fragment (377.07 Da). Taken together, the kinetic and spectroscopic data support the following mechanism for lactide ROP with **2**/$Cp_2Co$ (Scheme 2). We propose that catalyst activation occurs by ligand-based reduction of the dimer **2** to form the dimeric radical anion $\mathbf{2}^{\bullet-}$ (step 1). As indicated by the half-order in [Zn], the active catalyst is generated by dissociation into a monomeric Zn species. Rather than breaking up dimer $\mathbf{2}^{\bullet-}$ in a symmetric fashion, its dissociation into the anion $[LZn(OPh)_2]^-$ (**A**) and neutral $L^{\bullet}Zn$ (**B**) (step 2) is supported by crystallography and mass analysis. The isolated zincate **A** (as the $Cp^*_2Co^+$ salt) was inactive in lactide ROP, suggesting that **B** is involved in catalysis. The flexible coordination properties

**Scheme 2. Proposed Mechanism for the Formation of cPLA**

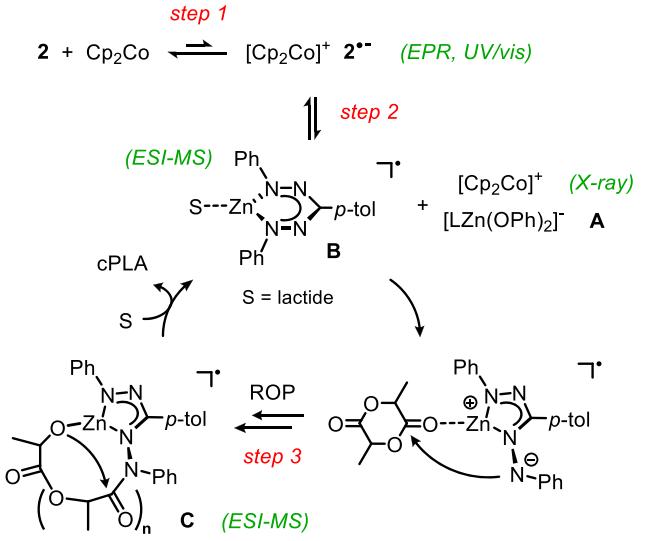


of the nitrogen-rich ligand allow liberation of the terminal N atom,[29] which can attack the coordinated lactide (step 3) to give a ligand-bound growing polymer chain in the form of a macrocyclic intermediate (**C**). Building on the early work of Kricheldorf et al.,[30] several catalysts are now known to form cyclic polymers via this "ring-expansion" pathway.[16a,b]

Finally, the reversibility of redox-switching was evaluated. Addition of $Cp_2Co$ (~1 equiv per Zn) to a $CD_2Cl_2$ solution of **2** resulted in a substantial shift and broadening of the $^1H$ NMR signals of the formazanate ligand (Figure S16). The resonances of the OPh moiety also broaden but remain in the same range ($\delta$ 6.4–7.0 ppm). Subsequent addition of 1 equiv of oxidant $[Cp_2Fe][PF_6]$ regenerates **2**, demonstrating that the redox chemistry of **2** is chemically reversible. This was corroborated in a catalysis experiment. An NMR tube containing a solution of **2** and 50 equiv of *rac*-lactide was monitored by $^1H$ NMR spectroscopy. As expected, no catalytic activity was observed in the absence of reducing agent, but the addition of 1 equiv of $Cp_2Co$ resulted in a linear increase in conversion (Figure 2).

After 1 h, a solution containing 1.05 equiv of $[Cp_2Fe][PF_6]$ was added, which completely halted the reaction. After another



https://doi.org/10.1021/acscatal.1c05689
ACS Catal. 2022, 12, 4125−4130

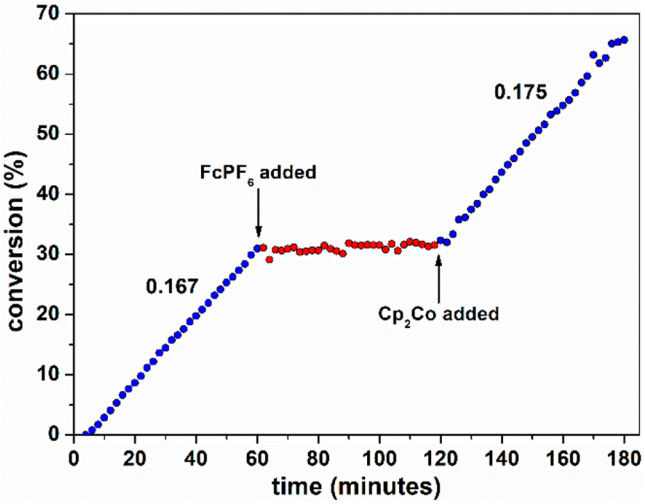


**Figure 2.** Conversion of lactide monitored by $^1$H NMR spectroscopy ($CD_2Cl_2$, 25 °C, $[LA]_0/[Zn]_0$ = 50, $[LA]_0$ = 0.5 M). $FcPF_6$ added after 60 min; $Cp_2Co$ added after 120 min. The numbers indicate the slope of the blue parts of the graph.

hour, the catalytic activity was fully restored by addition of 1.05 equiv of $Cp_2Co$. Thus, switching between "on" and "off" states occurs with excellent reversibility and a high $k_{on}/k_{off}$ ratio.[31] GPC analysis of samples taken throughout a redox-switching experiment shows that molecular weight increases linearly in the "on" period but is halted when in the "off" state, while dispersities remain low throughout ($Đ_M \approx 1.2$ for conversions < 70%).

In summary, we have demonstrated switchable ring-opening polymerization of *rac*-lactide with a formazanate zinc phenoxide complex. The kinetic and spectroscopic data confirm a key role for the ligand, not only in the redox activation but also as an initiator for the polymerization reaction and formation of cyclic PLA. The ready availability, tunability, and low cost of formazanate ligands make this an attractive platform for development of redox-switchable systems without being limited to the presence of a metal ion as the site of oxidation/reduction, and we anticipate that this could be more broadly applicable to achieve spatiotemporal control also for other catalytic reactions.

## ■ ASSOCIATED CONTENT

### Supporting Information

The Supporting Information is available free of charge at https://pubs.acs.org/doi/10.1021/acscatal.1c05689.

Experimental procedures and characterization data (PDF)

Crystallographic data for **A** (CIF)

Crystallographic data for **2** (CIF)

## ■ AUTHOR INFORMATION


### Corresponding Author

**Edwin Otten** − *Stratingh Institute for Chemistry, University of Groningen, 9747 AG Groningen, The Netherlands;* orcid.org/0000-0002-5905-5108; Email: edwin.otten@rug.nl

### Author

**Folkert de Vries** − *Stratingh Institute for Chemistry, University of Groningen, 9747 AG Groningen, The Netherlands*

Complete contact information is available at: https://pubs.acs.org/10.1021/acscatal.1c05689


### Notes

The authors declare no competing financial interest.

## ■ ACKNOWLEDGMENTS

We thank Albert J. J. Woortman for GPC analysis, Pieter van der Meulen for assistance with DOSY NMR spectroscopy and Renze Sneep for direct-injection ESI-MS measurements. Financial support from The Netherlands Organisation of Scientific Research (NWO) is gratefully acknowledged.

## ■ REFERENCES


(1) De Neve, J.; Haven, J. J.; Maes, L.; Junkers, T. Sequence-definition from controlled polymerization: the next generation of materials. *Polym. Chem.* **2018**, *9*, 4692−4705.

(2) (a) Leibfarth, F. A.; Mattson, K. M.; Fors, B. P.; Collins, H. A.; Hawker, C. J. External Regulation of Controlled Polymerizations. *Angew. Chem., Int. Ed.* **2013**, *52*, 199−210. (b) Blanco, V.; Leigh, D. A.; Marcos, V. Artificial switchable catalysts. *Chem. Soc. Rev.* **2015**, *44*, 5341−5370. (c) Teator, A. J.; Lastovickova, D. N.; Bielawski, C. W. Switchable Polymerization Catalysts. *Chem. Rev.* **2016**, *116*, 1969−1992. (d) Chen, C. Redox-Controlled Polymerization and Copolymerization. *ACS Catal.* **2018**, *8*, 5506−5514. (e) Doerr, A. M.; Burroughs, J. M.; Gitter, S. R.; Yang, X.; Boydston, A. J.; Long, B. K. Advances in Polymerizations Modulated by External Stimuli. *ACS Catal.* **2020**, *10*, 14457−14515.

(3) Lorkovic, I. M.; Duff, R. R.; Wrighton, M. S. Use of the Redox-Active Ligand 1,1′-Bis(diphenylphosphino)cobaltocene To Reversibly Alter the Rate of the Rhodium(I)-Catalyzed Reduction and Isomerization of Ketones and Alkenes. *J. Am. Chem. Soc.* **1995**, *117*, 3617−3618.

(4) Dechy-Cabaret, O.; Martin-Vaca, B.; Bourissou, D. Controlled Ring-Opening Polymerization of Lactide and Glycolide. *Chem. Rev.* **2004**, *104*, 6147−6176.

(5) Gregson, C. K. A.; Gibson, V. C.; Long, N. J.; Marshall, E. L.; Oxford, P. J.; White, A. J. P. Redox Control within Single-Site Polymerization Catalysts. *J. Am. Chem. Soc.* **2006**, *128*, 7410−7411.

(6) Wei, J.; Diaconescu, P. L. Redox-Switchable Ring-Opening Polymerization with Ferrocene Derivatives. *Acc. Chem. Res.* **2019**, *52*, 415−424.

(7) (a) Lowe, M. Y.; Shu, S.; Quan, S. M.; Diaconescu, P. L. Investigation of redox switchable titanium and zirconium catalysts for the ring opening polymerization of cyclic esters and epoxides. *Inorg. Chem. Front.* **2017**, *4*, 1798−1805. (b) Quan, S. M.; Wang, X.; Zhang, R.; Diaconescu, P. L. Redox Switchable Copolymerization of Cyclic Esters and Epoxides by a Zirconium Complex. *Macromolecules* **2016**, *49*, 6768−6778. (c) Wang, X.; Thevenon, A.; Brosmer, J. L.; Yu, I.; Khan, S. I.; Mehrkhodavandi, P.; Diaconescu, P. L. Redox Control of Group 4 Metal Ring-Opening Polymerization Activity toward l-Lactide and ε-Caprolactone. *J. Am. Chem. Soc.* **2014**, *136*, 11264−11267. (d) Hern, Z. C.; Quan, S. M.; Dai, R.; Lai, A.; Wang, Y.; Liu, C.; Diaconescu, P. L. ABC and ABAB Block Copolymers by Electrochemically Controlled Ring-Opening Polymerization. *J. Am. Chem. Soc.* **2021**, *143*, 19802−19808.

(8) (a) Biernesser, A. B.; Li, B.; Byers, J. A. Redox-controlled polymerization of lactide catalyzed by bis(imino)pyridine iron bis(alkoxide) complexes. *J. Am. Chem. Soc.* **2013**, *135*, 16553−16560. (b) Biernesser, A. B.; Delle Chiaie, K. R.; Curley, J. B.; Byers, J. A. Block Copolymerization of Lactide and an Epoxide Facilitated by a Redox Switchable Iron-Based Catalyst. *Angew. Chem., Int. Ed.* **2016**, *55*, 5251−5254.

(9) Sauer, A.; Buffet, J.-C.; Spaniol, T. P.; Nagae, H.; Mashima, K.; Okuda, J. Switching the Lactide Polymerization Activity of a Cerium Complex by Redox Reactions. *ChemCatChem.* **2013**, *5*, 1088−1091.
(10) Fang, Y.-Y.; Gong, W.-J.; Shang, X.-J.; Li, H.-X.; Gao, J.; Lang, J.-P. Synthesis and structure of a ferric complex of 2,6-di(1H-pyrazol-3-yl)pyridine and its excellent performance in the redox-controlled living ring-opening polymerization of ε-caprolactone. *Dalton Trans.* **2014**, *43*, 8282−8289.
(11) Doerr, A. M.; Burroughs, J. M.; Legaux, N. M.; Long, B. K. Redox-switchable ring-opening polymerization by tridentate ONN-type titanium and zirconium catalysts. *Catal. Sci. Technol.* **2020**, *10*, 6501−6510.
(12) (a) Anderson, W. C.; Rhinehart, J. L.; Tennyson, A. G.; Long, B. K. Redox-Active Ligands: An Advanced Tool To Modulate Polyethylene Microstructure. *J. Am. Chem. Soc.* **2016**, *138*, 774−777. (b) Delle Chiaie, K. R.; Biernesser, A. B.; Ortuño, M. A.; Dereli, B.; Iovan, D. A.; Wilding, M. J. T.; Li, B.; Cramer, C. J.; Byers, J. A. The role of ligand redox non-innocence in ring-opening polymerization reactions catalysed by bis(imino)pyridine iron alkoxide complexes. *Dalton Trans.* **2017**, *46*, 12971−12980. (c) Ortuño, M. A.; Dereli, B.; Chiaie, K. R. D.; Biernesser, A. B.; Qi, M.; Byers, J. A.; Cramer, C. J. The Role of Alkoxide Initiator, Spin State, and Oxidation State in Ring-Opening Polymerization of ε-Caprolactone Catalyzed by Iron Bis(imino)pyridine Complexes. *Inorg. Chem.* **2018**, *57*, 2064−2071.
(13) (a) Cheng, M.; Attygalle, A. B.; Lobkovsky, E. B.; Coates, G. W. Single-Site Catalysts for Ring-Opening Polymerization: Synthesis of Heterotactic Poly(lactic acid) from rac-Lactide. *J. Am. Chem. Soc.* **1999**, *121*, 11583−11584. (b) Chamberlain, B. M.; Cheng, M.; Moore, D. R.; Ovitt, T. M.; Lobkovsky, E. B.; Coates, G. W. Polymerization of Lactide with Zinc and Magnesium β-Diiminate Complexes: Stereocontrol and Mechanism. *J. Am. Chem. Soc.* **2001**, *123*, 3229−3238.
(14) (a) Chisholm, M. H.; Huffman, J. C.; Phomphrai, K. Monomeric metal alkoxides and trialkyl siloxides: (BDI)Mg(OtBu)-(THF) and (BDI)Zn(OSiPh3)(THF). Comments on single site catalysts for ring-opening polymerization of lactides. *J. Chem. Soc., Dalton Trans.* **2001**, 222−224. (b) Chisholm, M. H.; Gallucci, J.; Phomphrai, K. Coordination Chemistry and Reactivity of Monomeric Alkoxides and Amides of Magnesium and Zinc Supported by the Diiminato Ligand CH(CMeNC6H3−2,6-iPr2)2. A Comparative Study. *Inorg. Chem.* **2002**, *41*, 2785−2794.
(15) Gilroy, J. B.; Otten, E. Formazanate coordination compounds: synthesis, reactivity, and applications. *Chem. Soc. Rev.* **2020**, *49*, 85−113.
(16) (a) Kricheldorf, H. R. Cyclic polymers: Synthetic strategies and physical properties. *J. Polym. Sci., Part A: Polym. Chem.* **2010**, *48*, 251−284. (b) Chang, Y. A.; Waymouth, R. M. Recent progress on the synthesis of cyclic polymers via ring-expansion strategies. *J. Polym. Sci., Part A: Polym. Chem.* **2017**, *55*, 2892−2902. (c) Haque, F. M.; Grayson, S. M. The synthesis, properties and potential applications of cyclic polymers. *Nat. Chem.* **2020**, *12*, 433−444.
(17) de Vries, F.; Travieso-Puente, R.; Roewen, P.; Otten, E. Three-Coordinate Zinc Methyl Complexes with Sterically Demanding Formazanate Ligands. *Organometallics* **2021**, *40*, 63−71.
(18) Duda, A.; Kowalski, A. Chapter 1: Thermodynamics and Kinetics of Ring-Opening Polymerization. *Handbook of Ring-Opening Polymerization* **2009**, 1−51.
(19) (a) Aubrecht, K. B.; Hillmyer, M. A.; Tolman, W. B. Polymerization of Lactide by Monomeric Sn(II) Alkoxide Complexes. *Macromolecules* **2002**, *35*, 644−650. (b) Zhong, Z.; Dijkstra, P. J.; Feijen, J. Controlled and Stereoselective Polymerization of Lactide: Kinetics, Selectivity, and Microstructures. *J. Am. Chem. Soc.* **2003**, *125*, 11291−11298. (c) Williams, W. K.; Breyfogle, L. E.; Choi, S. K.; Nam, W.; Young, V. G., Jr; Hillmyer, M. A.; Tolman, W. B. A Highly Active Zinc Catalyst for the Controlled Polymerization of Lactide. *J. Am. Chem. Soc.* **2003**, *125*, 11350−11359. (d) Moravek, S. J.; Messman, J. M.; Storey, R. F. Polymerization kinetics of rac-lactide initiated with alcohol/stannous octoate using in situ attenuated total reflectance-fourier transform infrared spectroscopy: An initiator study. *J. Polym. Sci. A Polym. Chem.* **2009**, *47*, 797−803. (e) Stasiw, D. E.; Luke, A. M.; Rosen, T.; League, A. B.; Mandal, M.; Neisen, B. D.; Cramer, C. J.; Kol, M.; Tolman, W. B. Mechanism of the Polymerization of rac-Lactide by Fast Zinc Alkoxide Catalysts. *Inorg. Chem.* **2017**, *56*, 14366−14372.
(20) (a) Bassi, M. B.; Padias, A. B.; Hall, H. K. The hydrolytic polymerization of ε-caprolactone by triphenyltin acetate. *Polym. Bull.* **1990**, *24*, 227−232. (b) Ding, K.; Miranda, M. O.; Moscato-Goodpaster, B.; Ajellal, N.; Breyfogle, L. E.; Hermes, E. D.; Schaller, C. P.; Roe, S. E.; Cramer, C. J.; Hillmyer, M. A.; Tolman, W. B. Roles of Monomer Binding and Alkoxide Nucleophilicity in Aluminum-Catalyzed Polymerization of ε-Caprolactone. *Macromolecules* **2012**, *45*, 5387−5396. (c) Huang, Y.; Wang, W.; Lin, C.-C.; Blake, M. P.; Clark, L.; Schwarz, A. D.; Mountford, P. Potassium, zinc, and magnesium complexes of a bulky OOO-tridentate bis(phenolate) ligand: synthesis, structures, and studies of cyclic ester polymerisation. *Dalton Trans.* **2013**, *42*, 9313−9324.
(21) Normand, M.; Dorcet, V.; Kirillov, E.; Carpentier, J.-F. {Phenoxy-imine}aluminum versus -indium Complexes for the Immortal ROP of Lactide: Different Stereocontrol, Different Mechanisms. *Organometallics* **2013**, *32*, 1694−1709.
(22) (a) van Strijdonck, G. P. F.; Boele, M. D. K.; Kamer, P. C. J.; de Vries, J. G.; van Leeuwen, P. W. N. M. Fast Palladium Catalyzed Arylation of Alkenes Using Bulky Monodentate Phosphorus Ligands. *Eur. J. Inorg. Chem.* **1999**, *1999*, 1073−1076. (b) Rosner, T.; Le Bars, J.; Pfaltz, A.; Blackmond, D. G. Kinetic Studies of Heck Coupling Reactions Using Palladacycle Catalysts: Experimental and Kinetic Modeling of the Role of Dimer Species. *J. Am. Chem. Soc.* **2001**, *123*, 1848−1855. (c) Burés, J. A Simple Graphical Method to Determine the Order in Catalyst. *Angew. Chem., Int. Ed.* **2016**, *55*, 2028−2031. (d) Davis-Gilbert, Z. W.; Wen, X.; Goodpaster, J. D.; Tonks, I. A. Mechanism of Ti-Catalyzed Oxidative Nitrene Transfer in [2 + 2 + 1] Pyrrole Synthesis from Alkynes and Azobenzene. *J. Am. Chem. Soc.* **2018**, *140*, 7267−7281.
(23) GPC analysis of samples taken at different time intervals during polymerization (with conversions <70%) indicate significantly lower $Đ_M$ of ca. 1.2 (Figure S33). The larger $Đ_M$ values at high conversion are ascribed to transesterification reactions that become competitive when lactide monomer is depleted.
(24) Connelly, N. G.; Geiger, W. E. Chemical Redox Agents for Organometallic Chemistry. *Chem. Rev.* **1996**, *96*, 877−910.
(25) Neither the β-diketiminate Zn catalyst of Coates, (BDI)ZnO$^i$Pr, nor *rac*-lactide give any detectable EPR signal when treated under the same conditions with $Cp_2Co$.
(26) (a) Ohki, Y.; Murata, A.; Imada, M.; Tatsumi, K. C-H Bond Activation of Decamethylcobaltocene Mediated by a Nitrogenase Fe8S7 P-Cluster Model. *Inorg. Chem.* **2009**, *48*, 4271−4273. (b) MacLeod, K. C.; McWilliams, S. F.; Mercado, B. Q.; Holland, P. L. Stepwise N−H bond formation from N2-derived iron nitride, imide and amide intermediates to ammonia. *Chem. Sci.* **2016**, *7*, 5736−5746.
(27) Broere, D. L. J.; Mercado, B. Q.; Lukens, J. T.; Vilbert, A. C.; Banerjee, G.; Lant, H. M. C.; Lee, S. H.; Bill, E.; Sproules, S.; Lancaster, K. M.; Holland, P. L. Reversible Ligand-Centered Reduction in Low-Coordinate Iron Formazanate Complexes. *Chem. Eur. J.* **2018**, *24*, 9417−9425.
(28) (a) Barbon, S. M.; Price, J. T.; Reinkeluers, P. A.; Gilroy, J. B. Substituent-Dependent Optical and Electrochemical Properties of Triarylformazanate Boron Difluoride Complexes. *Inorg. Chem.* **2014**, *53*, 10585−10593. (b) Chang, M.-C.; Dann, T.; Day, D. P.; Lutz, M.; Wildgoose, G. G.; Otten, E. The Formazanate Ligand as an Electron Reservoir: Bis(Formazanate) Zinc Complexes Isolated in Three Redox States. *Angew. Chem., Int. Ed.* **2014**, *53*, 4118−4122. (c) Chang, M. C.; Otten, E. Synthesis and ligand-based reduction chemistry of boron difluoride complexes with redox-active formazanate ligands. *Chem. Commun.* **2014**, *50*, 7431−7433.
(29) (a) Travieso-Puente, R.; Chang, M.-C.; Otten, E. Alkali metal salts of formazanate ligands: diverse coordination modes as a result of the nitrogen-rich [NNCNN] ligand backbone. *Dalton Trans.* **2014**,


https://doi.org/10.1021/acscatal.1c05689
*ACS Catal.* 2022, 12, 4125−4130

*43*, 18035−18041. (b) Chang, M.-C.; Roewen, P.; Travieso-Puente, R.; Lutz, M.; Otten, E. Formazanate Ligands as Structurally Versatile, Redox-Active Analogues of *β*-Diketiminates in Zinc Chemistry. *Inorg. Chem.* **2015**, *54*, 379−388. (c) Kabir, E.; Mu, G.; Momtaz, D. A.; Bryce, N. A.; Teets, T. S. Formazanate Complexes of Bis-Cyclometalated Iridium. *Inorg. Chem.* **2019**, *58*, 11672−11683.

(30) (a) Kricheldorf, H. R.; Lee, S.-R. Polylactones. 35. Macrocyclic and Stereoselective Polymerization of.beta.-D,L-Butyrolactone with Cyclic Dibutyltin Initiators. *Macromolecules* **1995**, *28*, 6718−6725. (b) Kricheldorf, H. R.; Lee, S.-R.; Bush, S. Polylactones 36. Macrocyclic Polymerization of Lactides with Cyclic Bu2Sn Initiators Derived from 1,2-Ethanediol, 2-Mercaptoethanol, and 1,2-Dimercaptoethane. *Macromolecules* **1996**, *29*, 1375−1381.

(31) See the Supporting Information for additional switching cycles (Figure S34) and a demonstration of the stability of the system in the "off" state (Figure S18).



https://doi.org/10.1021/acscatal.1c05689
*ACS Catal.* 2022, 12, 4125−4130